International Journal of Current Research and Techniques (IJCRT)
Volume 16, Issue 1, 2026; DOI: 10.5281/ZENODO.19023091
Original Research Article

Research on Splicing Technology of Expressway Reconstruction and Expansion Based on Finite Element Method

Haoran Gu, *School of Civil Engineering, Guangzhou University, Guangzhou 510006, China.*

Wenke Huang *, *School of Civil Engineering, Guangzhou University, Guangzhou 510006, China.*

***Corresponding Author: Wenke Huang (W.H)**

Manuscript Received: Mar 09, 2026; Revised: Mar 15, 2026; Published: Mar 15, 2026

Abstract: To address the mechanical performance issues of the splicing structure between new and old pavements in expressway reconstruction and expansion projects, this study employed ABAQUS software based on the three-dimensional continuum finite element method to systematically analyze the effects of load magnitude, layer modulus, and number of steps on the interlayer stress of the spliced pavement. The research findings can provide theoretical basis for the splicing design and construction control of highway widening and reconstruction projects.

Keywords: Highway Widening and Reconstruction; Finite Element Analysis; Splicing of New and Old Pavements; Mechanical Response.

1. Introduction

As the core backbone of the comprehensive transportation system, expressways play an irreplaceable strategic role in promoting coordinated regional economic development and improving logistics and transportation efficiency[1], [2]. With the gradual improvement of China's expressway network, early-constructed expressways generally face issues such as saturated traffic capacity and declining service levels[3]. Consequently, reconstruction and expansion have become important technical means for enhancing highway performance[4]. However, in expansion projects, the splicing area between new and old pavements is prone to induce distresses such as reflective cracking, interlayer slippage, and differential settlement due to structural discontinuity, and uncoordinated settlement deformation, which severely compromise pavement performance and traffic safety[5], [6], [7] .

Mechanical performance analysis of the splicing structure between new and old pavements is critical for optimizing design and preventing distresses[8], [9]. ABAQUS, with its capability to simulate material nonlinearity, geometric discontinuity, and multi-condition loading scenarios, serves as an important tool for structural mechanical analysis[10], [11]. A certain expressway section in Guangdong Province has been in operation for over ten years, originally designed as a four-lane dual carriageway. Due to year-by-year increases in traffic volume, this expressway is now operating under overload conditions, and an expansion project to upgrade it to an eight-lane dual carriageway is planned. Based on this context, this study takes a certain expressway reconstruction and expansion project as the research object, establishes a finite element model using ABAQUS, investigates the influence patterns of load position, load level, material modulus, and the number of steps on the mechanical performance of the spliced pavement, determines the most unfavorable load condition, evaluates the numerical values of mechanical indicators at each layer interface, and proposes optimization design recommendations. The findings aim to provide theoretical reference for the splicing structure design and construction quality control of expressway reconstruction and expansion projects[12], [13].

2. Development of Pavement Model

2.1. Model Parameters

The pavement structure of a certain expressway reconstruction and expansion project is shown in Figure 1 (with a total lapping width of 1.5 m). Based on the pavement structure of the subgrade section, a finite element model was established as illustrated in Figure 1. To simplify the calculation, several assumptions were made as follows:

(1) Each structural layer is continuous, perfectly elastic, homogeneous, and isotropic.

(2) Model dimensions: 15 m (cross-section) ×12 m (driving direction) ×5.26 m (total thickness);

(3) Constraint settings: Complete fixation applied to the bottom of the subgrade, the side surfaces are constrained only for horizontal displacement perpendicular to the surface, and the top surface is unconstrained.

(4) The tire-pavement contact area is idealized as a rectangle of 16 cm×22 cm, with a dual-wheel center spacing of 32 cm. The load magnitude is 0.7 MPa, and the right edge of the load in the vertical direction coincides with the contact surface between the new and old subgrades;

(5) Interface bonding condition between new and old pavements: complete contactt

Each structural layer was discretized using 3D solid elements (C3D8R solid reduced integration elements). Free meshing was adopted for the mesh density. The model contains 344,885 elements and 381,699 nodes. The material parameters are listed in Table 1

Table 1. Material Parameters

Pavement Structure	Elastic Modulus（MPa）	Poisson's Ratio
SMA-13	12000	0.25
GAC-20	12000	0.25
ATB-25	11000	0.25
Cement-Stabilized Macadam	22000	0.25
Graded Crushed Stone	400	0.35
AC-13	12850	0.25
AC-20	12850	0.25
AC-25	12850	0.25
Aged Cement-Stabilized Macadam	9250	0.25
Old Subgrade	125	0.35
New Subgrade	60	0.35

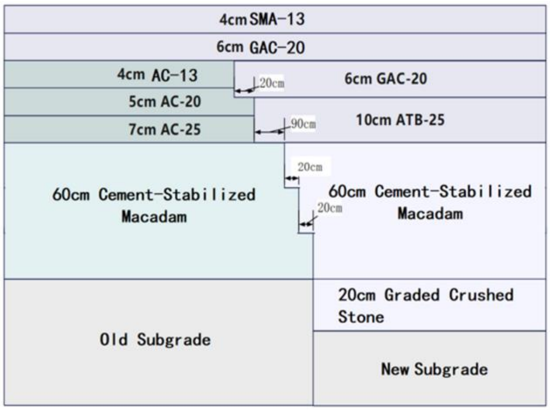

(a)Schematic Diagram of Pavement Structure Combination

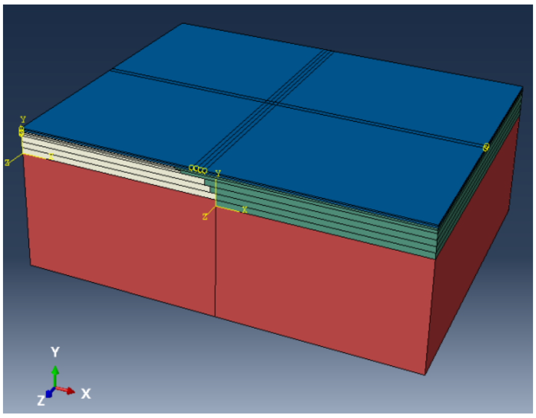

(b) Finite Element Model of Pavement Structure

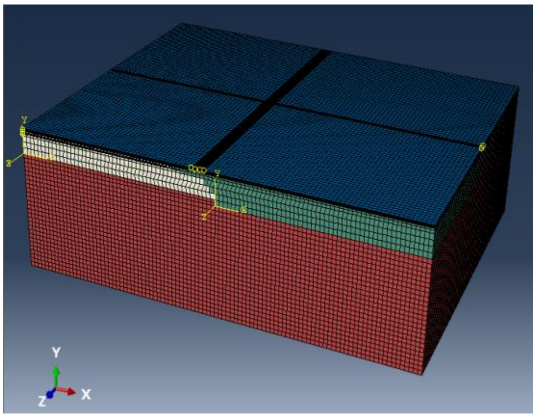

(c)Mesh Generation

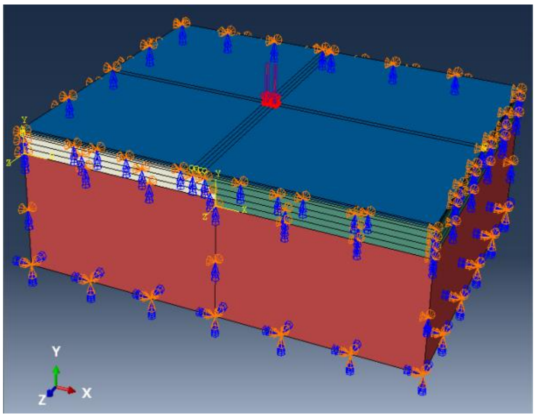

(d)Boundary Conditions and Loading

Figure 1. Schematic diagram of pavement structure

2.2. Feasibility Verification

The rationality of the established pavement structure finite element model was verified by comparing the calculated surface deflection of the model with the measured surface deflection[14]. The calculated vertical surface deflection was 5.16 (0.01 mm), which is close to the average measured deflection value of 5.59 (0.01 mm) at the center point of the FWD falling weight, proving the rationality of the established pavement structure finite element model.

3. Analysis of Factor Effects on Stress Characteristics of Pavement Splicing Structure Layers

3.1. Analysis of Different Load Effects

Vehicle overloading has long been one of the primary causes of highway damage in China[15]. In recent years, due to intensified crackdown efforts on overloading, the phenomenon has improved to some extent[16], [17]; however, it remains widespread.herefore, Therefore, the impact of overloading on the widened pavement structure is a key research focus[18].The present study investigates the impact of load level variation on pavement structural behavior [19], with four load magnitudes considered: 0.7 MPa, 1.0 MPa, 1.2 MPa, and 1.5 MPa. The load positions are illustrated in Figure 2.

The asphalt layer stress and strain responses under the four load levels are illustrated in Figure 3. As evident from the figure, both stress and strain increase linearly with increasing load. When the load reaches 1.5 MPa, the calculated values are 2.14 times those under the standard load of 0.7 MPa. Similarly, with increasing load, various stresses and strains in the base layer (Figure 4) also increase linearly. When the load reaches 1.5 MPa, their calculated values are also 2.14 times those under the standard load of 0.7 MPa.

Excessive load levels may lead to structural damage of the spliced pavement. Since all analysis indicators of the pavement structure vary linearly with increasing load, when the load reaches 1.2 MPa, the asphalt surface layer reaches its tensile strength limit,furthermore, the shear stress within the asphalt layer approaches its shear strength limit under elevated load levels. Consequently, the contact pressure of passing vehicles should be strictly limited to 1.2 MPa to prevent premature pavement distress induced by heavy overloads.

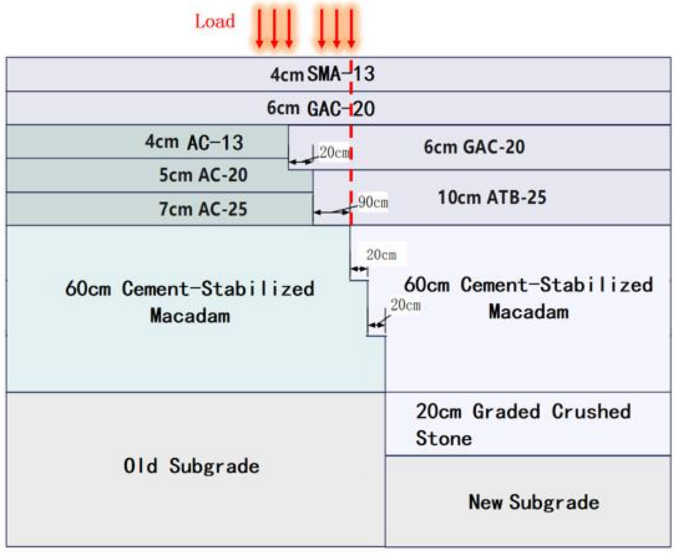

Figure 2. Load Position

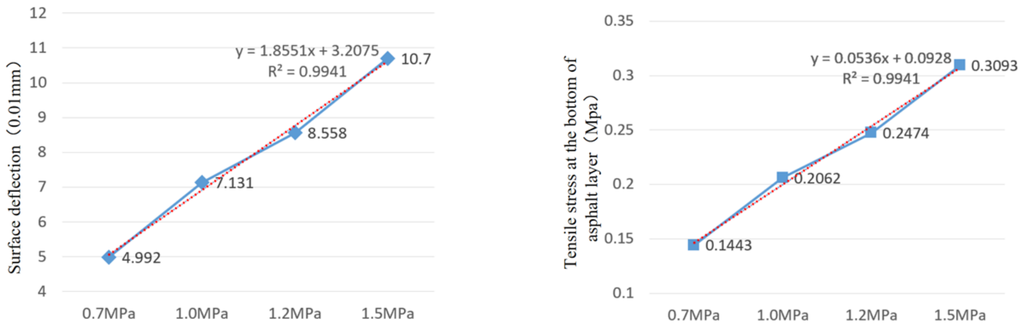

(a)Surface deflection (b)Tensile stress at the bottom of asphalt layer

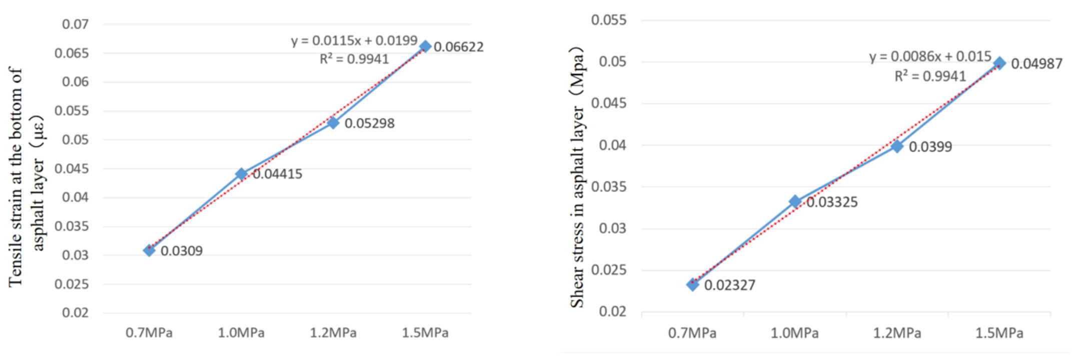

(c) Tensile strain at the bottom of asphalt layer (d)Shear stress in asphalt layer

Figure 3. Stress and Strain of Asphalt Layer under Different Conditions

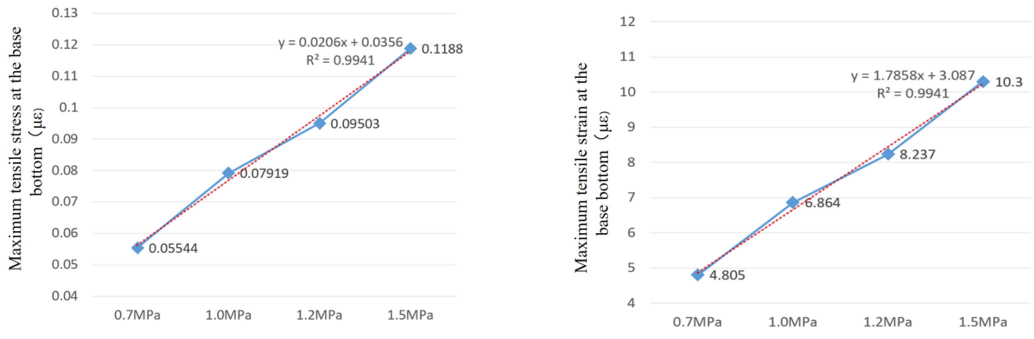

(a)Maximum tensile stress at the base bottom (b)Maximum tensile strain at the base bottom

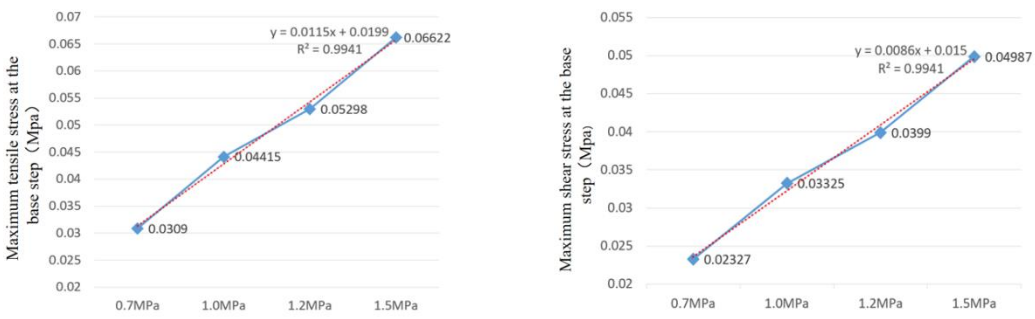

(c)Maximum tensile stress at the base step (d)Maximum shear stress at the base step

Figure 4. Stress and Strain of Base Layer under Different Conditions

3.2. Analysis of Modulus Effects

The modulus difference between new and old pavements is also one of the key causes of distress in reconstructed and expanded roads, significantly affecting the structural stress, deformation coordination, and long-term service performance of the pavement[20], [21].This study investigated the effects of modulus variation in the new asphalt surface layer, new base layer, and cement-stabilized crushed stone base on pavement structural response through parametric analyses involving reduction of the new surface and base layer moduli to 0.7 times their baseline values, reduction of the old surface and base layer moduli to 0.7 times their baseline values, increase of the new surface and base layer moduli by factors of 1.3, 1.5, 2.0, and 3.0, and reduction of the subgrade modulus to 20 MPa and 40 MPa from a baseline of 60 MPa. The specific modulus adjustment multipliers are summarized in Table 2.

Table 2. Modulus multiple

Pavement Structure	Elastic Modulus（MPa）							Poisson's Ratio
	0.7times (Old)	0.7times (new)	Base	1.3times (new)	1.5times (new)	2times (new)	3times (new)	
SMA-13	-	8400	12000	15600	18000	24000	36000	0.25
GAC-20	-	8400	12000	15600	18000	24000	36000	0.25
ATB-25	-	7700	11000	14300	16500	22000	33000	0.25
Cement-Stabilized Macadam	-	15400	22000	28600	33000	44000	66000	0.25
Graded Crushed Stone	-	-	400	-	-	-	-	0.35
AC-13	8995	-	12850	-	-	-	-	0.25
AC-20	8995	-	12850	-	-	-	-	0.25
AC-25	8995	-	12850	-	-	-	-	0.25
Aged Cement-Stabilized Macadam	6475	-	9250	-	-	-	-	0.25
Old Subgrade	-	-	125	-	-	-	-	0.35
New Subgrade	-	-	60	-	-	-	-	0.35

（1）Different Modulus Multiples

The asphalt layer stress-strain responses under varying modulus multiples are presented in Figure 5. Reducing new layer moduli to 0.7 times increased surface deflection, asphalt bottom tensile stress, and asphalt bottom tensile strain by 17.3%, 6.3%, and 46.2%, respectively, with negligible shear stress variation, indicating compromised deflection resistance and fatigue performance. Conversely, modulus increases of 1.3 to 3.0 times significantly reduced surface deflection (by 10.6% to 36.5%) and asphalt bottom tensile strain (by 24.3% to 68.4%), while tensile and shear stresses remained stable. Thus, moderate modulus enhancement improves deformation resistance and fatigue life. However, the beneficial effects gradually diminish once the modulus increase exceeds 1.3 times, indicating that pursuing modulus ratios beyond this threshold yields diminishing returns and is not cost-effective.

Reduction in the moduli of the old surface and base layers induces only minor stress and strain variations in the asphalt layer relative to the benchmark scenario, suggesting that modulus degradation of the existing pavement structure has limited bearing on the overlying asphalt layer's structural integrity.

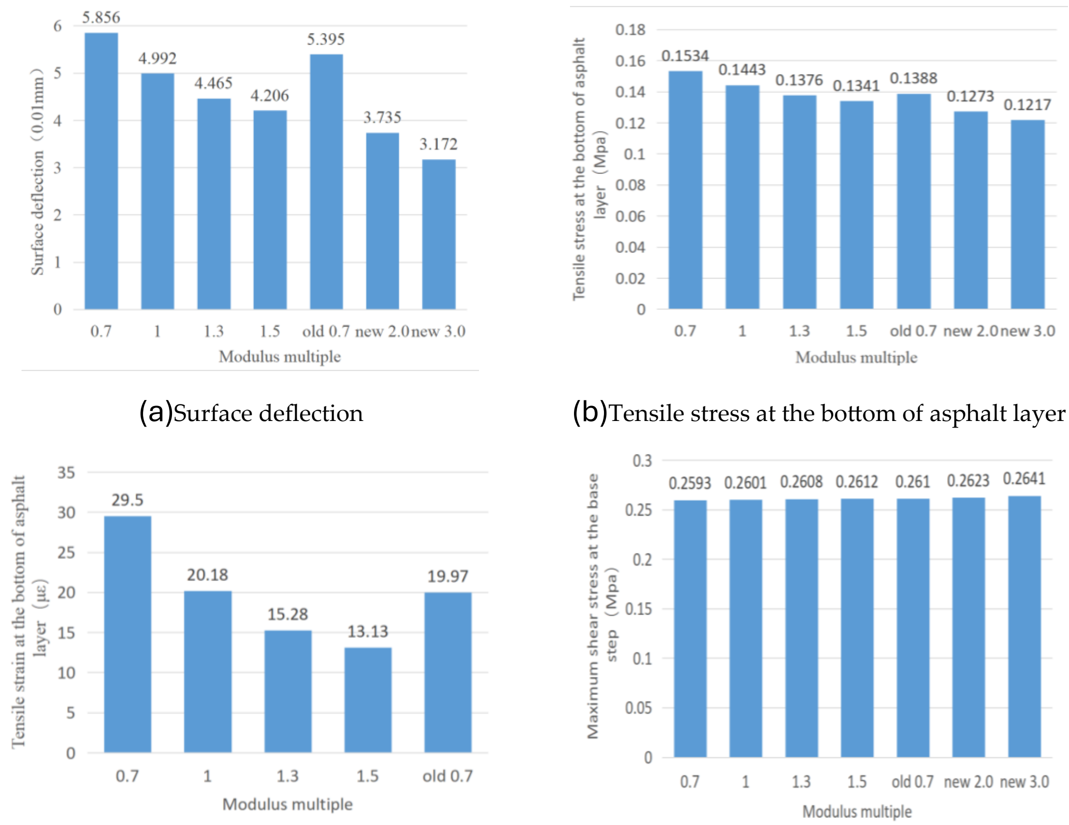

(a)Surface deflection (b)Tensile stress at the bottom of asphalt layer

(c) Tensile strain at the bottom of asphalt layer (d)Shear stress in asphalt layer

Figure 5. Stress and Strain of Asphalt Layer under Different Conditions

The base layer stress and strain distributions under varying modulus multiples are presented in Figure 6. Reducing new layers moduli to 0.7 times increases base bottom tensile stress and strain, and base step tensile and shear stress by 8.7%, 7.9%, 10.1%, and 4.9%, respectively, adversely affecting base layer stress and strain states, with limited influence on base step shear stress.

When the moduli of the new surface and base layers increase, the stress and strain in the base layer exhibit a decreasing trend. However, it is noteworthy that when the modulus increases by 1.5 times, the reduction amplitudes of stress and strain indicators—such as the maximum tensile stress at the base bottom—remain relatively modest, with decreases of merely 10.2%, 9.4%, 12.7%,and 7.6%, respectively. When the modulus increases by 3 times, the calculated indicators for the base layer, interface, and subgrade top achieve reduction magnitudes ranging from 25% to 35%. Nevertheless, relying on increasing the moduli of the new surface and base layers to enhance deformation resistance and fatigue life does not align with economic efficiency.

Old layer modulus attenuation (to 0.7 times original values) decreased base bottom maximum tensile stress, base interface tensile stress, and base bottom maximum tensile strain by 14.6%, 19%, and 6.8%, respectively, beneficially alleviating tensile stress concentrations. However, base bottom maximum tensile strain increased by 23.7%, adversely affecting base layer fatigue resistance and exacerbating subgrade compressive plastic deformation.

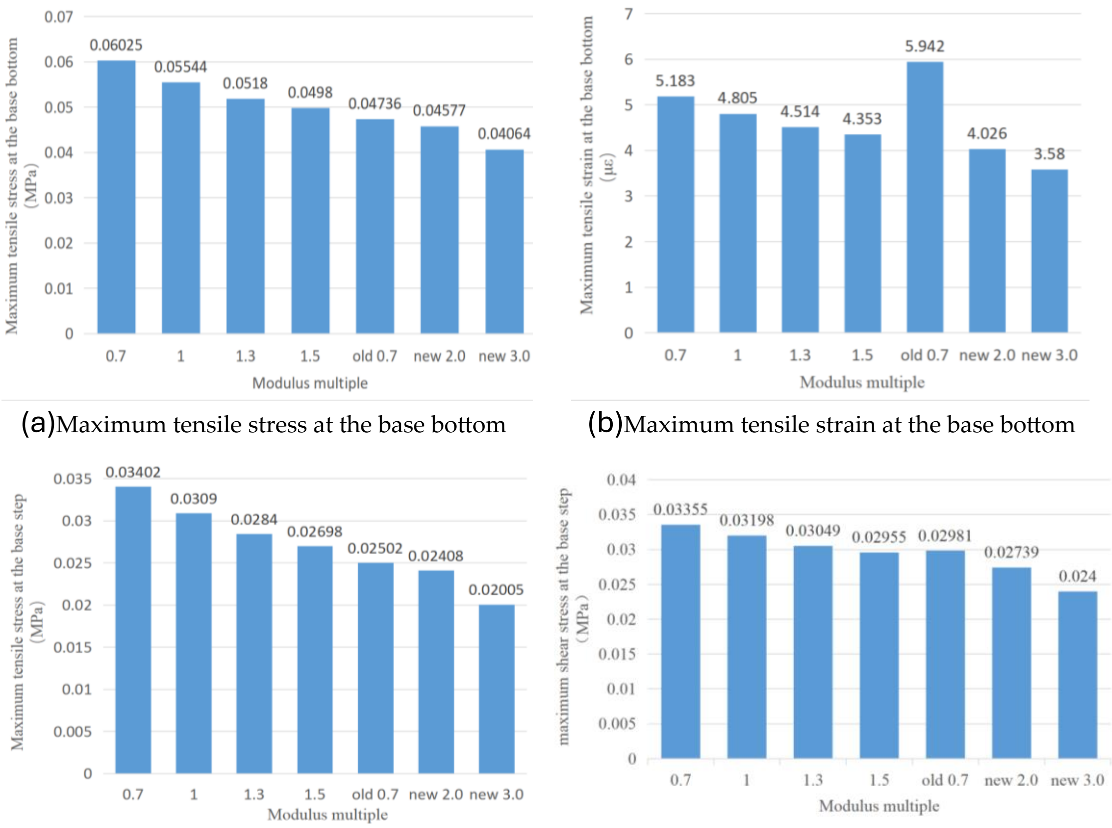

(a)Maximum tensile stress at the base bottom (b)Maximum tensile strain at the base bottom

(c)Maximum tensile stress at the base step (d)Maximum shear stress at the base step

Figure 6. Stress and Strain of Base Layer under Different Conditions

（2）Reducing the modulus of new subgrade

The calculation results for reducing the modulus of new subgrade to 20 MPa and 40 MPa (with the baseline modulus of 60 MPa) are shown in Figures 7, 8. As indicated in the figures, reducing the modulus of new subgrade has limited influence on various analysis indicators of the pavement structure. However, it should be noted that a smaller modulus of new subgrade implies non-uniform compaction of the subgrade, posing a risk of significant post-construction settlement.

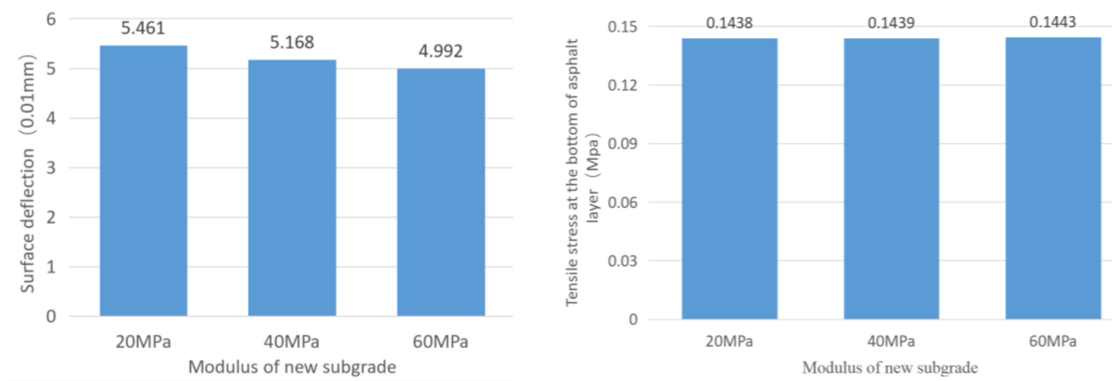

(a)Surface deflection (b)Tensile stress at the bottom of asphalt layer

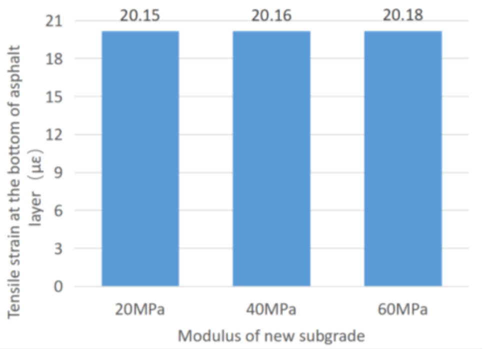

(c) Tensile strain at the bottom of asphalt layer

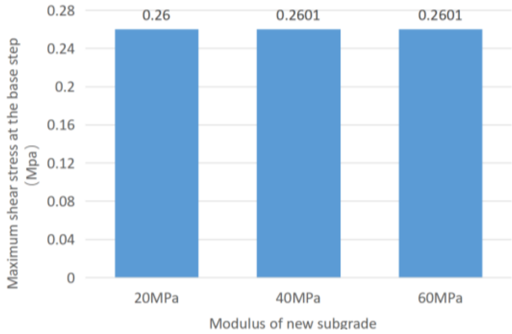

(d)Shear stress in asphalt layer

Figure 7. Stress and Strain of Asphalt Layer under Different Conditions

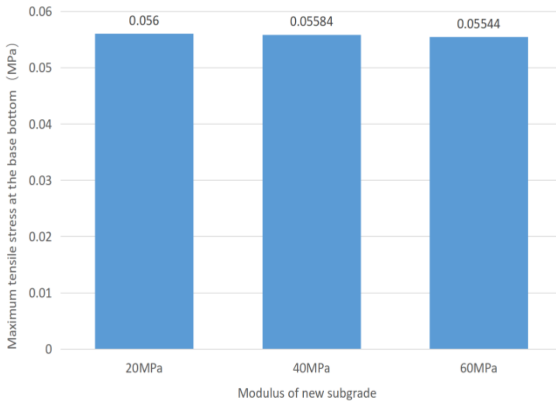

(a)Maximum tensile stress at the base bottom

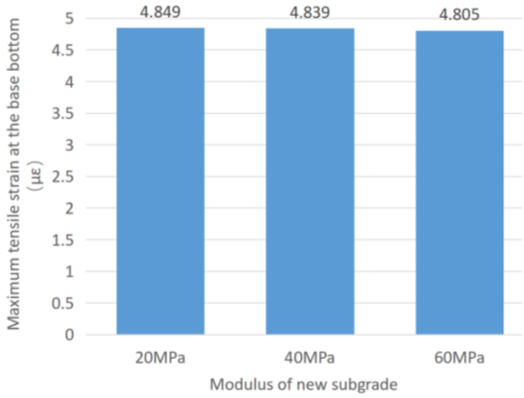

(b)Maximum tensile strain at the base bottom

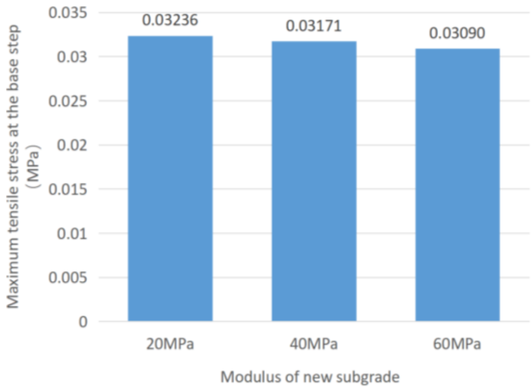

(c)Maximum tensile stress at the base step

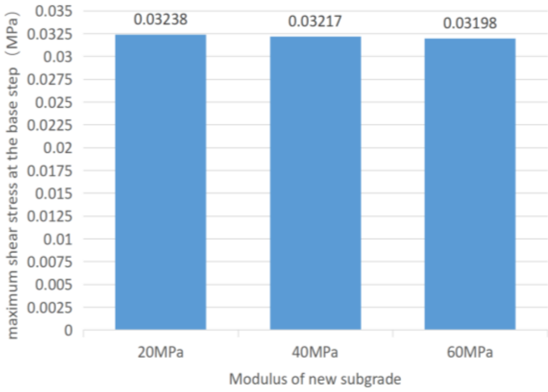

(d)Maximum shear stress at the base step

Figure 8. Stress and Strain of Base Layer under Different Conditions

3.3 Analysis of Step Number Effects

The lapping step at the longitudinal joint of a spliced pavement creates localized stress concentrations, generating excessive tensile strains at the overlay bottom that ultimately initiate premature cracking[22], [23]. This section analyzes the influence of five step quantities on the stress and strain distributions within each layer of the pavement structure, with the specific step configurations illustrated in Figure 9. The load positions remain consistent with those described previously.

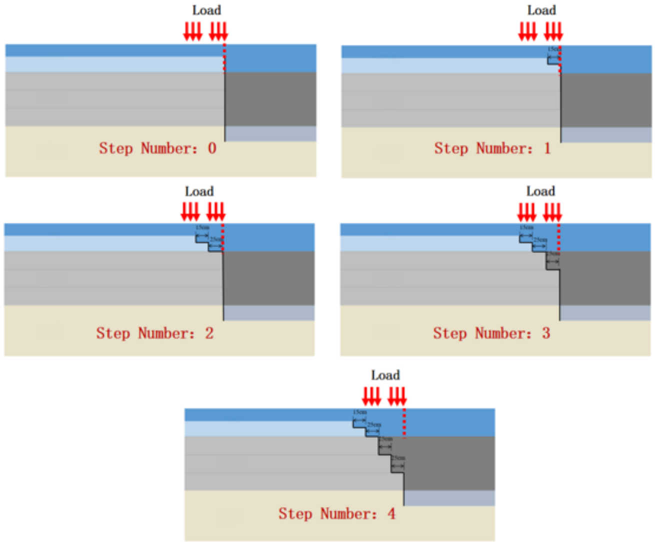

Figure 9. Configuration of Step Numbers

The calculated stress and strain results of the asphalt layer under five step configurations are presented in Figure 10. As shown in the figure, setting steps in the surface layer significantly reduces the stress and strain in the asphalt layer. Although setting steps in the base layer is unfavorable to surface deflection, it effectively reduces the tensile strain at the bottom of the asphalt layer and the shear stress within the layer.

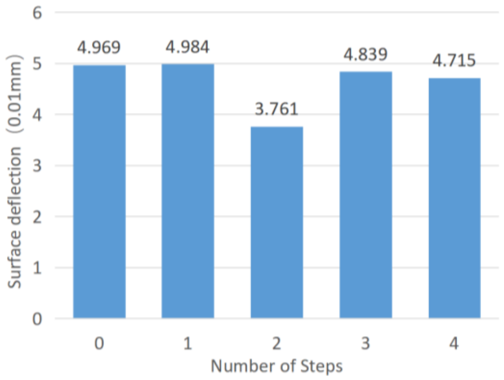

(a)Surface deflection

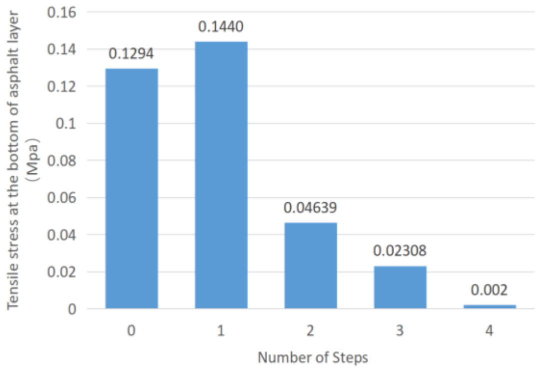

(b)Tensile stress at the bottom of asphalt layer

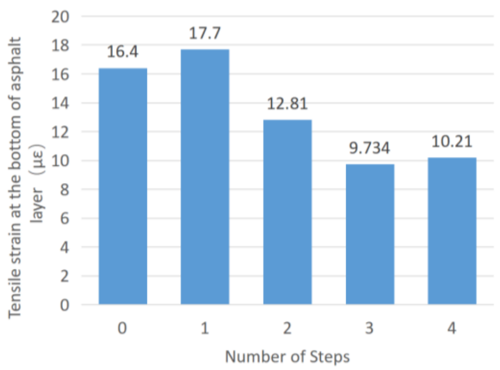

(c) Tensile strain at the bottom of asphalt layer

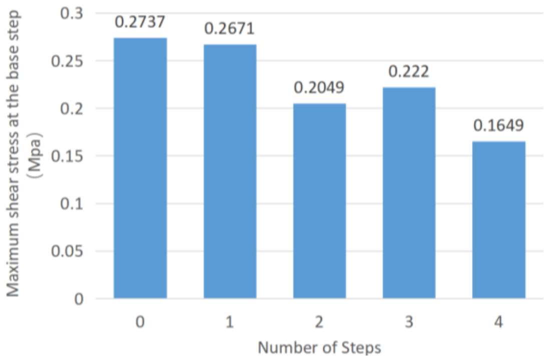

(d)Shear stress in asphalt layer

Figure 10. Surface deflection; tensile stress at the bottom of asphalt layer; tensile strain at the bottom of asphalt layer; shear stress in asphalt layer

The calculation results of stress and strain for each base level under 5 different numbers of steps are shown in Figure 11. As illustrated, from the surface layer step perspective, a single step exerts negligible influence compared with the no-step case; however, increasing to two steps reduces the maximum tensile stress, tensile strain, and shear stress at the base bottom and base step by 22.7%, 24.5%, 27.4%, and 33.7%, respectively. From the base layer step perspective:

although step introduction moderately increases the maximum tensile stress and strain at the base bottom and base step, the magnitudes remain limited; conversely, increasing base layer step quantities significantly reduces the maximum shear stress at the base step.

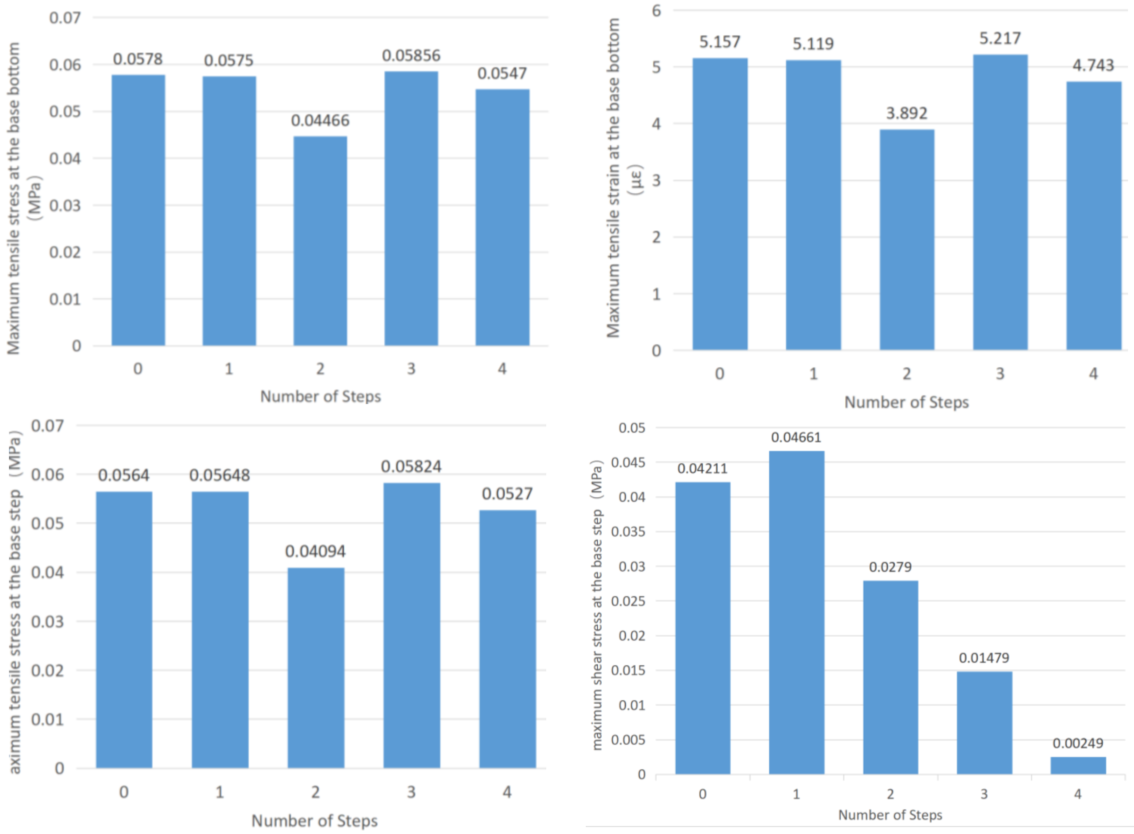

Figure 11. Stress and Strain of Base Layer under Different Conditions

4. Conclusions

(1) Various analysis indicators of the pavement structure change linearly with increasing load. When the load reaches 1.2 MPa, the asphalt surface layer reaches its tensile strength limit, and the shear strength of the asphalt layer also approaches its shear strength limit. Therefore, the load of passing vehicles should be strictly limited to 1.2 MPa to avoid early damage to the pavement caused by a large number of overloaded vehicles.

(2) Reducing new layer moduli increases asphalt bottom tensile strain and surface deflection, compromising fatigue resistance and ride comfort, with negligible effects on other indicators. Old layer modulus decay reduces base bottom and interfacial tensile stresses favorably yet impairs base fatigue resistance and exacerbates subgrade plastic deformation. Conversely, increasing new layer moduli effectively mitigates asphalt bottom tensile strain, enhancing fatigue resistance. Nevertheless, improving the moduli of the new surface and base layers by more than 1.3 times to achieve only marginal improvements in mechanical performance does not satisfy economic efficiency criteria.

Since setting the number of steps in both the surface layer and base layer to 2 (i.e., total of 4 steps) yields the maximum reduction in maximum shear stress at the base step, it is recommended to set 2 steps in the surface layer and 2 steps in the base layer, respectively.

5.References

[1] C. Davis and M. K. Jha, “Modeling the Effects of Socioeconomic Factors in Highway Construction and Expansion,” J. Transp. Eng., vol. 135, no. 12, pp. 990–998, Dec. 2009, doi: 10.1061/(ASCE)0733-947X(2009)135:12(990).

[2] C. Liu, C. Liu, W. Peng, and W. Wang, “Infrastructure, financial access, and economic growth: evidence from a quasi-experiment in China,” Oxf. Econ. Pap., vol. 78, no. 1, pp. 68–89, Jan. 2026, doi: 10.1093/oep/gpaf022.

[3] S. Wang, F. Niu, J. Chen, and Y. Dong, “Permafrost research in China related to express highway construction,” Permafr. Periglac. Process., vol. 31, no. 3, pp. 406–416, Jul. 2020, doi: 10.1002/ppp.2053.

[4] S. Alexander, B. Yang, and O. Hussey, “Examining the Land Use and Land Cover Impacts of Highway Capacity Expansions in California Using Remote Sensing Technology,” Transp. Res. Rec. J. Transp. Res. Board, vol. 2679, no. 2, pp. 439–449, Feb. 2025, doi: 10.1177/03611981241262299.

[5] W. Wu, H. Zhang, Z. Liu, and Y. Wang, “Numerical Analysis on Transverse Splicing Structure for the Widening of a Long Multi-Span Highway Concrete Continuous Box Girder Bridge,” Materials, vol. 15, no. 19, p. 6805, Sep. 2022, doi: 10.3390/ma15196805.

[6] Y. Li, Z. Zou, J. Zhang, and Y. He, “Study on the evolution of airport asphalt pavement integrated distress based on association rule mining,” Constr. Build. Mater., vol. 369, p. 130565, Mar. 2023, doi: 10.1016/j.conbuildmat.2023.130565.

[7] H. Yu, Y. Wang, and Y. Chen, “Causes of cracking of an existing pavement after highway widening in an area of soft soil,” Proc. Inst. Civ. Eng. - Transp., vol. 175, no. 3, pp. 168–177, Jun. 2022, doi: 10.1680/jtran.18.00171.

[8] Q. Wang, B. Zhou, Q. Wu, K. Chen, D. Lai, and Z. Liang, “Mechanical behavior analysis of concrete girder bridges widened by partial splicing method,” Struct. Concr., p. suco.70338, Sep. 2025, doi: 10.1002/suco.70338.

[9] Y. Fu et al., “Mechanical behaviour of concrete pavement widening,” Road Mater. Pavement Des., vol. 25, no. 4, pp. 678–693, Apr. 2024, doi: 10.1080/14680629.2023.2221351.

[10] S. B. Carici and J. Oner, “Application of finite element method in highway base and subbase layers,” Matér. Rio Jan., vol. 30, p. e20250346, 2025, doi: 10.1590/1517-7076-rmat-2025-0346.

[11] K.-C. Fu and F. Lu, “Nonlinear Finite-Element Analysis for Highway Bridge Superstructures,” J. Bridge Eng., vol. 8, no. 3, pp. 173–179, May 2003, doi: 10.1061/(ASCE)1084-0702(2003)8:3(173).

[12] Y. Liu, “Dynamic Response and Deformation Characteristics of Urban Loess Subgrade under Vehicle Loading,” Soil Mech. Found. Eng., vol. 62, no. 1, pp. 80–87, Mar. 2025, doi: 10.1007/s11204-025-10030-2.

[13] C. Si et al., “Dynamic Response Analysis of Rutting Resistance Performance of High Modulus Asphalt Concrete Pavement,” Appl. Sci., vol. 8, no. 12, p. 2701, Dec. 2018, doi: 10.3390/app8122701.

[14] P.-Q. Xia and J. M. W. Brownjohn, “Bridge Structural Condition Assessment Using Systematically Validated Finite-Element Model,” J. Bridge Eng., vol. 9, no. 5, pp. 418–423, Sep. 2004, doi: 10.1061/(ASCE)1084-0702(2004)9:5(418).

[15] Z. Xu, Q. Han, J. Jia, Z. Zhong, and C. Huang, “Evaluation of a current vehicle load model using weigh-in-motion records: a case in China,” Balt. J. Road Bridge Eng., vol. 11, no. 3, pp. 197–204, Sep. 2016, doi: 10.3846/bjrbe.2016.23.

[16] Y. Liu, D. Li, Z. Zhang, H. Zhang, and N. Jiang, “Fatigue Load Model Using the Weigh-in-Motion System for Highway Bridges in China,” J. Bridge Eng., vol. 22, no. 6, p. 04017011, Jun. 2017, doi: 10.1061/(ASCE)BE.1943-5592.0001048.

[17] P. Lou, H. Nassif, D. Su, and P. Truban, “Effect of Overweight Trucks on Bridge Deck Deterioration Based on Weigh-in-Motion Data,” Transp. Res. Rec. J. Transp. Res. Board, vol. 2592, no. 1, pp. 86–97, Jan. 2016, doi: 10.3141/2592-10.

[18] H. Li, J. Wekezer, and L. Kwasniewski, “Dynamic Response of a Highway Bridge Subjected to Moving Vehicles,” J. Bridge Eng., vol. 13, no. 5, pp. 439–448, Sep. 2008, doi: 10.1061/(ASCE)1084-0702(2008)13:5(439).

[19] S. Wang et al., “Load Identification of High-Speed Train Crossbeam Based on Bayesian Finite Element Model Updating and Load-Strain Linear Superposition Algorithm,” IEEE Sens. J., vol. 23, no. 12, pp. 13489–13498, Jun. 2023, doi: 10.1109/JSEN.2023.3270161.

[20] M. Kim and E. Tutumluer, “Validation of a Three-Dimensional Finite Element Model using Airfield Pavement Multiple Wheel Load Responses,” Road Mater. Pavement Des., vol. 11, no. 2, pp. 387–408, Jan. 2010, doi: 10.1080/14680629.2010.9690281.

[21] O. Ü. Bayrak and S. Hınıslıoğlu, “A new approach to the design of rigid pavement: single-axle loading,” Road Mater. Pavement Des., vol. 18, no. 3, pp. 573–589, May 2017, doi: 10.1080/14680629.2016.1182056.

[22] S. Yaqoob, J. Silfwerbrand, and R. G. R. Balieu, “A Parametric Study Investigating the Dowel Bar Load Transfer Efficiency in Jointed Plain Concrete Pavement Using a Finite Element Model,” Buildings, vol. 14, no. 4, p. 1039, Apr. 2024, doi: 10.3390/buildings14041039.

[23] S. Li, Y. Niu, B. Wang, Y. Gao, and Y. Zhu, “Research on Mechanical Response of Polymer Grouting Repair for Longitudinal Cracks in Reconstructed and Expanded Expressway Pavement,” Math. Probl. Eng., vol. 2022, pp. 1–8, Apr. 2022, doi: 10.1155/2022/5760674.